ENGINEERING TRANSACTIONS • *Engng. Trans.* • **54**, 3, 223–231, 2006
Polish Academy of Sciences • Institute of Fundamental Technological Research
10.24423/engtrans.419.2006

DYNAMIC EFFECTS OF MATERIAL DAMPING IN ACTIVE LAMINATES REINFORCED WITH PIEZOCERAMIC FIBERS

M. Pietrzakowski

Institute of Machine Design Fundamentals
Warsaw University of Technology
Warsaw, Poland
e-mail: mpi@simr.pw.edu.pl

In the paper rectangular, simply supported, laminated plates composed of classical fiber-reinforced layers and active layers of piezoelectric properties are under consideration. The aim of the study is to determine the influence of anisotropic passive damping on the active vibration reduction achieved and the sensitivity of the system to material axes' orientation of piezocomposite actuator layers. The effects of piezoceramic fiber direction and passive damping intensity are illustrated by means of the amplitude-frequency characteristics.

Key words: active laminate, piezocomposite, piezoceramic fiber, material damping.

1. Introduction

Active composite structures with embedded piezoelectric fibers offer a great potential in modern technical implementations known as intelligent structures. The determination of electro-mechanical properties of such structures is of importance for the engineering design and control effectiveness obtained. Early theoretical studies and experiments were reported by Clark *et al.* [3] and Bogacz and Popp [2] among others. The studies addressed to the control applications were presented by Lee [4], Mitchell and Reddy [5] and Reddy [9], in which the constitutive equations of piezoelectric laminates are derived using the classical and shear deformation of laminated plate theories. The idea of using active composites reinforced with piezoceramic fibers has been presented by Bent and Hagood [1], who also have formulated the constitutive equations for a new generation of piezoelectric fiber composites equipped with interdigitated electrodes (IDEFC). The modelling of laminated plates with such piezocomposite layers and a comparison of structural vibration control effectiveness depending on the piezocomposite configuration including the fiber direction and distribution scheme, the fiber volume fraction and the poling direction applied, were discussed by Pietrzakowski [6, 8] and Pietrzakowski and Tylikowski [7]. The aim of this study is to recognise the influence of passive material damping

with anisotropic properties on the structural vibration control. The rectangular, simply supported, laminated plates composed of conventional fiber-reinforced layers (e.g. graphite-epoxy) and active layers of piezoelectric properties are under consideration. The IDEPFC layers are used as actuators. This type of hybrid composite with aligned in-plane axially polarized PZT (lead-zirconate-titanate) ceramic fibers offers an increase of the predominant unidirectional actuation effect as compared with traditionally electroded piezocomposites supplied with electric field along their thickness. The IDEPFC actuator layers and the PVDF (polyvinylidene fluoride) polymeric sensor layers operate in a closed loop, realising the velocity feedback. The effective properties of the diphase composite material (PZT ceramic and polymeric matrix) are obtained due to the uniform field method by combining the material phases properties according to the rule of mixtures and assuming the uniform mechanical and electric fields within each material phase (cf. BENT and HAGOOD [1]). The effects of material axes' orientation of viscoelastic piezocomposite layers on the active vibration reduction achieved are discussed and illustrated by means of amplitude-frequency characteristics.

2. FORMULATION OF THE PROBLEM

In the case under consideration of symmetrically laminated, specially orthotropic plates, the bending-stretching coupling vanishes and the bending-twisting coupling can be ignored. Hence, the controlled transverse motion $w(x,y,t)$ of the plate subjected to the external harmonic excitation $q(x,y,t)$ and the control loading $p(x,y,t)$ can be described by

$$D_{11}\frac{\partial^4 w}{\partial x^4} + 2\left(D_{12}+2D_{66}\right)\frac{\partial^4 w}{\partial x^2 \partial y^2} + D_{22}\frac{\partial^4 w}{\partial y^4} + \tilde{\rho}\,\frac{\partial^2 w}{\partial t^2} = q\left(x,y,t\right) - p\left(x,y,t\right) \tag{2.1}$$

with

$$p\left(x,y,t\right) = \frac{\partial^2 M_x}{\partial x^2} + \frac{\partial^2 M_y}{\partial y^2} + 2\frac{\partial^2 M_{xy}}{\partial x \partial y}$$

where: D_{ij} – elements of the bending stiffness matrix $\mathbf{D}$, $i,\ j = 1,2,6$, $\tilde{\rho}$ – mass density parameter, M_x, M_y, M_{xy} – control moment components distributed along the edges of the activated area.

The control moment resultant is generated due to the reverse piezoelectric effect, and for the laminate composed of n actuator layers and supplied with

averaged electric field $E_3^{(k)}$, it has the form

$$\mathbf{M} = [M_x,\ M_y,\ M_{xy}]^T = \sum_{k=1}^{n} [C_1,\ C_2,\ C_6]_{(k)}^T E_3^{(k)} z_0^{(k)} \lambda(x,y) \tag{2.2}$$

where: $z_0^{(k)}$ – distance of the k-th active layer from the laminate midplane, λ – pattern function of the activated area, C_i – actuator layer constants with respect to the x, y plate axes, $i = 1, 2, 6$.

$$[C_1,\ C_2,\ C_6]_{(k)}^T = t_a \mathbf{R}^{(k)} \mathbf{e}^{\mathrm{ef}}.$$

In the above equation the effective electromechanical coupling matrix $\mathbf{e}^{\mathrm{ef}} = [e_{33}^{\mathrm{ef}},\ e_{31}^{\mathrm{ef}},\ 0]^T$ is determined according to the uniform fields method by considering the representative volume element. Symbol t_a indicates the actuator layer thickness. The transformation matrix $\mathbf{R}^{(k)}$ relates to the angle between the material axes of the k-th active layer and the plate reference axes.

Naturally, to generate the control bending loading, midplane symmetric actuators of the same polarization direction have to be supplied with the opposite electric fields. The actuator interaction (Eq. (2.2)) can be expressed in relation to the applied voltage after substituting the electric field-voltage formula $E_3(t) = V(t)/l_p$. The symbol l_p denotes the average length of electric field paths between the interdigitated electrode sections. The path length l_p can be approximated by the relation $l_p = d + t_a(1 - v_2^p)$ depending on the electrode spacing d, layer thickness t_a and piezoelectric material fraction measured along the thickness v_2^p.

The voltage $V(t)$ is produced by sensor layers due to their mechanical deformation and transformed according to the velocity feedback rule with the constant gain factor. The sensor equation is formulated based on the constitutive law of direct piezoelectric effect. In the considered case, the sensors are monolithic PVDF layers of the thickness t_s covered by traditional surface electrodes. After integrating the charge stored and using the standard equation for capacitance, the voltage $V^{(k)}$ produced by the k-th sensor is given as

$$V^{(k)}(t) = -\frac{z_0^{(k)} t_s}{\in_{33} S^{(k)}} \mathbf{R}^{(k)} \mathbf{e}^T \int_0^a \int_0^b \left[\frac{\partial^2 w}{\partial x^2},\ \frac{\partial^2 w}{\partial x^2},\ 2\frac{\partial^2 w}{\partial x \partial y}\right]^T \lambda_s(x,y)\, dx\, dy \tag{2.3}$$

where: a, b – midplane dimensions of the laminate, λ_s – pattern function of the electrode, $S^{(k)}$ – effective electrode area, $\in_{33}$ – permittivity constant, $\mathbf{e}$ – piezoelectric coefficient matrix of the PVDF, $\mathbf{e} = [e_{31},\ e_{32},\ 0]^T$.

Details of the actuator and sensor relations can be found in the papers by PIETRZAKOWSKI [6, 8].

The properties of material components (fiber and matrix) and design parameters such as fiber direction and fiber volume fraction, create anisotropic nature of the effective material properties including material damping. Viscoelastic behaviour of the laminate is approximated according to the Voigt–Kelvin model. Modelling of inner energy dissipation is based on the elastic-viscoelastic correspondence principle to predict complex moduli for fiber-reinforced composites, which in general can be written in the form

$$E_{ii}^{*} = E_{ii}\,(1 + j\mu_{ii}\omega)\,(i = 1, 2), \qquad G_{12}^{*} = G_{12}\,(1 + j\mu_{12}\omega)\,, \tag{2.4}$$

where μ_{ii} denote the retardation time parameters for tension/compression in the material orthotropy directions, respectively, and μ_{12} is the retardation time associated with in-plane shear.

The viscoelastic properties of classic layers and active layers (piezocomposite and monolithic) are considered separately according to the micromechanical models, and the complex stiffness matrices $\mathbf{c}_{(k)}^{*}$ for each layer are derived. The global stiffness matrix of the laminate is combined of the averaged effective properties of the layers and for the bending effect is given by the formula

$$\mathbf{D}^{*} = \frac{1}{3}\sum_{k=1}^{n} \bar{\mathbf{c}}_{(k)}^{*}\left(z_k^3 - z_{k-1}^3\right), \tag{2.5}$$

where the complex stiffness matrix $\bar{\mathbf{c}}_{(k)}^{*}$ refers to the k-th ply of thickness $t_k = z_k - z_{k-1}$ and is determined with respect to the plate reference axes x, y.

The result of modelling of the viscoelastic behaviour is the complex form of the elements of the laminate bending stiffness matrix $\mathbf{D}^{*}$.

The solution to the equation of motion, Eq. (2.1), with simply supported boundary conditions is obtained for the steady-state case and expressed in terms of the frequency response functions.

3. Results and discussion

Calculations are performed for a simply supported laminated plate of the dimensions $400\times400\times1.75$ mm and composed of classical graphite-epoxy layers and sensor/actuator layers. The symmetric stacking sequence $[90°/\mathrm{A}^{+}/\mathrm{A}^{-}/S^{+}/0°]_s$ is applied. The symbols "A" and "S" indicate the actuator and sensor, respectively, and the upper scripts "+" and "−" give the sign of the inclination angle θ with respect to the x-axis of the plate. The stiffness parameters of the graphite-epoxy composite are the following: $E_{11} = 150$ GPa, $E_{22} = 9$ GPa, $G_{12} = 7.1$ GPa

and the equivalent mass density is equal to $\rho = 1600$ kg/m^3. The electromechanical properties of piezoelectric composite components are listed in Table 1 (cf. BENT and HAGOOD, [1]).

Table 1. Properties of PFC components.

Parameter	ρ kgm^{-3}	c_{11} GPa	c_{12} GPa	c_{13} GPa	c_{33} GPa	G GPa	e_{31} Cm^{-2}	e_{33} Cm^{-2}	ϵ_{33} / ϵ_0
PZT-5H	7650	127	80.2	84.7	117	36.3	–4.42	15.5	1392
Matrix	1200	8.15	4.01	4.01	8.15	2.33	0	0	11.2

The uniform PZT fiber distribution with the volume fraction of $v_f = 0.25$ and the ratio of electrode spacing to layer thickness $d/t_a = 6$ for IDEPFC actuators is assumed. The properties of PVDF material are the following: $E = 2$ GPa, $\rho = 1780$ kg/m^3, piezoelectric constants $d_{31} = 2.3 \cdot 10^{-11}$ mV^{-1}, $d_{32} = 3 \cdot 10^{-12}$ mV^{-1}. The sensor and actuator layers operate in a common closed loop with velocity feedback of the constant gain $k_d = 0.4$ s. Internal damping is based on the Voigt–Kelvin model with the following parameters (retardation times): $\mu_1 = 10^{-6}$ s, $\mu_2 = \mu_{12} = 4 \cdot 10^{-6}$ s for orthotropic graphite-epoxy layers, $\mu_p = 2 \cdot 10^{-6}$ s for mechanically isotropic PVDF layers and $\mu_m = 8 \cdot 10^{-6}$ s for matrix material in piezocomposite layers. The values of damping constants are based on experimental results presented by VANTOMME [10]. Energy dissipation in ceramic PZT fibers is ignored. The above parameters define material damping which is further called the actual damping. It should be underlined that the damping parameters are assumed to be independent of the frequency and this simplification can be a source of errors, especially for composite materials demonstrating a relatively strong passive damping.

The harmonic excitation of the amplitude intensity $q_0 = 1$ Nm^{-2} is uniformly distributed over the plate surface. Due to the laminate architecture, the stiffness matrix elements responsible for bending-twisting coupling (D_{16} and D_{26}) are small enough compared with others, and a globally orthotropic behaviour of the laminate can be assumed.

Numerical simulations are performed to show the influence of anisotropic passive damping on active vibration reduction and also the sensitivity of the system to material axes' orientation of active layers.

The modification of dynamic responses created by a different passive damping level and the PZT fiber reorientation for the first (1–1) mode, the consecutive resonance relating to the 3–1 mode and the 1–3 mode are shown in Fig. 1, Fig. 2 and Fig 3, respectively.

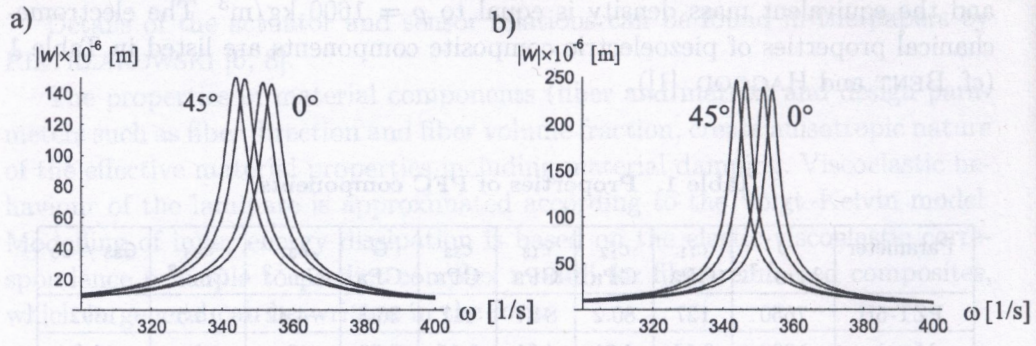

FIG. 1. Influence of the PZT fiber direction on the 1–1 vibration mode. Effect of material damping changes: a) actual damping, b) 10 times stronger damping.

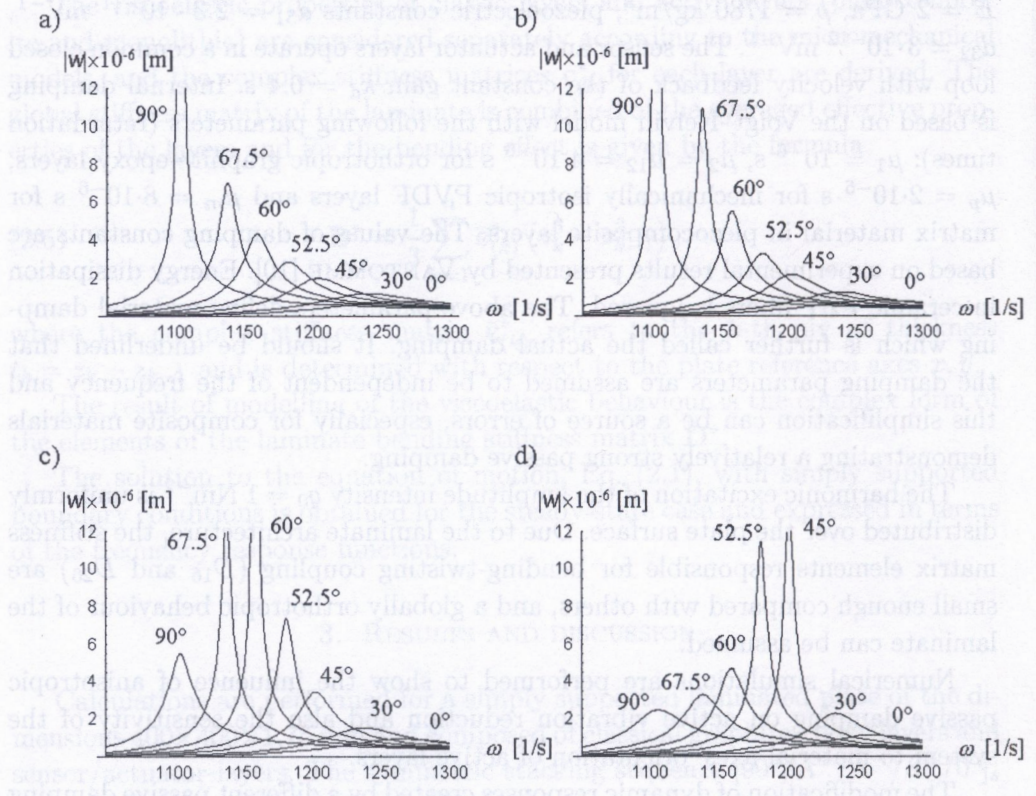

FIG. 2. Influence of the PZT fiber direction on the 3–1 vibration mode. Effect of material damping changes: a) 10 times weaker damping, b) actual damping, c) 4 times stronger damping, d) 8 times stronger damping.

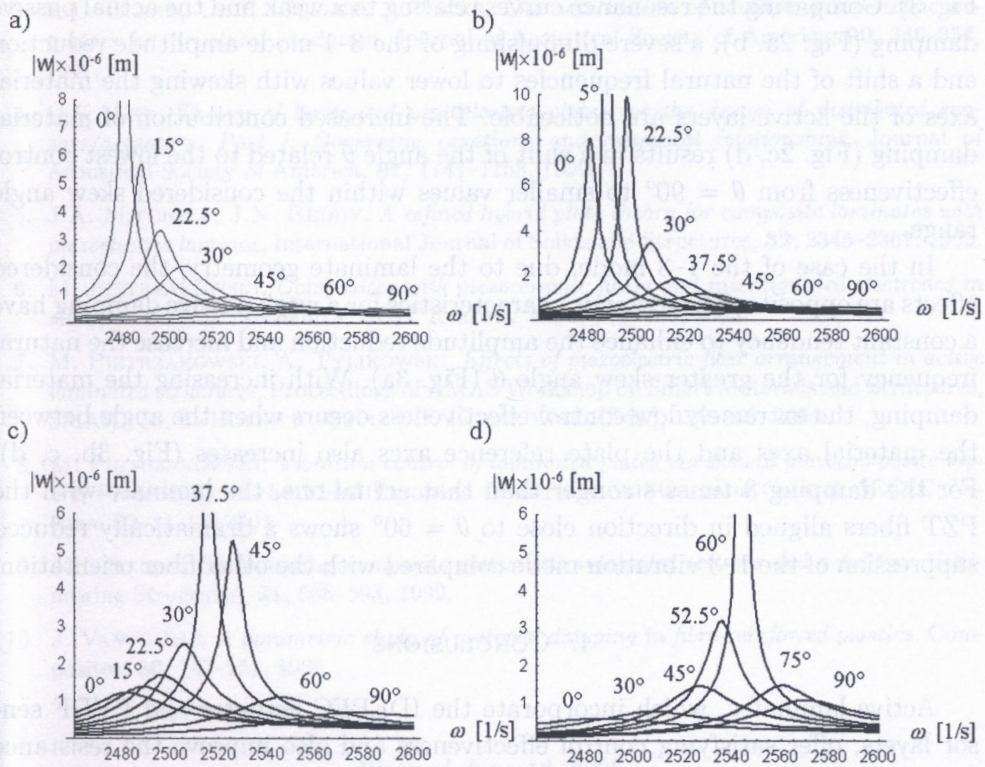

FIG. 3. Influence of the PZT fiber direction on the 1–3 vibration mode. Effect of material damping changes: a) 10 times weaker damping, b) actual damping, c) 4 times stronger damping, d) 8 times stronger damping.

The amplitude-frequency characteristics are calculated at point $x = y = 100$ mm. The changes in passive damping relate to the actual damping defined above and they are determined by a multiplication factor common for all the material components of the laminate.

In the case of the 1–1 mode the PZT fiber reorientation from 0° to 45° results in a slight increase of the resonance amplitude (Fig. 1), which occurs at lower frequencies. A further increase in the angle θ changes the results and then the cycle repeats. A decrease of the control effectiveness is observed within the range of a relatively strong material damping because of a reduction of the signal generated by the sensor (Fig. 1b). Of course, for an extremely strong passive damping the vibration suppression is intensified.

The effects of the PZT fiber direction on the 3–1 mode and the next 1–3 mode are covered by the angle θ variation between 0° and 90° (Fig. 2 and

Fig. 3). Comparing the resonance curves relating to a weak and the actual passive damping (Fig. 2a, b), a severe diminishing of the 3–1 mode amplitude reduction and a shift of the natural frequencies to lower values with skewing the material axes of the active layers are noticeable. The increased contribution of material damping (Fig. 2c, d) results in a shift of the angle θ related to the lowest control effectiveness from $\theta = 90°$ to smaller values within the considered skew angle range.

In the case of the 1–3 mode, due to the laminate geometry, the considered effects are opposite. The dynamic characteristics for a weak passive damping have a constant tendency to enhance the amplitude reduction and increase the natural frequency for the greater skew angle θ (Fig. 3a). With increasing the material damping, the extremely low control effectiveness occurs when the angle between the material axes and the plate reference axes also increases (Fig. 3b, c, d). For the damping 8 times stronger than that actual one, the laminate with the PZT fibers aligned in direction close to $\theta = 60°$ shows a dramatically reduced suppression of the 1–3 vibration mode compared with the other fiber orientation.

4. Conclusions

Active laminates, which incorporate the IDEPFC actuator and PVDF sensor layers, offer satisfying control effectiveness and also improve the resistance to damage by bending cracks. The primary piezoelectric effect applied into the plane of the structure improves the performance of active elements, also for modal control purposes. The capacity to intensify active suppression of particular vibration modes can be modified during the manufacturing process by adopting a suitable fiber direction related to the plate axes. The presented numerical examples present the effects of the material axes reorientation on both the resonance amplitudes and the natural frequencies. It should be underlined that the control effect strongly depends on passive energy dissipation, whose anisotropic nature is typical for fiber-reinforced composites. The combined active and passive forms of vibration reduction can, to a greater or lesser extent, disturb the expected skewing effect depending on the material damping level.

References

1. A. A. Bent, N.W. Hagood, *Piezoelectric fiber composites with interdigitated electrodes*, J. of Intell. Mater. Syst. and Struct., **8**, 903–919, 1997.

2. R. Bogacz, K. Popp, *On numerical simulation and experimental verification of behaviour of active control beam structure*, Proceedings of 2-nd Workshop of Polish Association of Computer Simulations "Simulation in Investigations and Development", R. Bogacz, Z. Osiński, J. Wróbel [Eds.], 35–44, 1995.

3. R.L. CLARC, CH.R. FULLER, A.WICKS, *Characterization of multiple piezoelectric actuators for structural excitation*, Journal of Acoustical Society of America, **90**, 346–357, 1991.

4. C.K. LEE, *Theory of laminated piezoelectric plates for the design of distributed sensors/actuators. Part I: Governing equations and reciprocal relationships*, Journal of Acoustical Society of America, **87**, 1144–1158, 1990.

5. J.A. MITCHELL, J.N. REDDY, *A refined hybrid plate theory for composite laminates with piezoelectric laminae*, International Journal of Solids and Structures, **32**, 2345–2367, 1995.

6. M. PIETRZAKOWSKI, *Composites with piezoceramic fibers and interdigitated electrodes in vibration control*, Mechanika, AGH, Kraków, **22**, 3, 375–380, 2003.

7. M. PIETRZAKOWSKI, A. TYLIKOWSKI, *Effects of piezoelectric fiber arrangement in active laminated structures*, Proceedings of AMAS Workshop on Smart Materials and Structures, SMART'03, J. HOLNICKI–SZULC, P. KOŁAKOWSKI [Eds.], 159–168, 2004.

8. M. PIETRZAKOWSKI, *Vibration control of laminated plates via skewed piezocomposite layers*, Proceedings of the Third European Conference on Structural Control, 3ECSC, Vienna, S2–14–17, 2004.

9. J.N. REDDY, *On laminated composite plates with integrated sensors and actuators*, Engineering Structures, **21**, 568–593, 1999.

10. J. VANTOMME, *A parametric study of material damping in fibre-reinforced plastics*, Composites, **26**, 147–151, 1995.

Received June 13, 2005.